Theor Chem Acc (2016) 135:51
DOI 10.1007/s00214-016-1811-2

REGULAR ARTICLE

Theoretical investigation on the reaction mechanism and kinetics of benzyl alcohol with OH radical

Cuihong Sun[1,2] · Liqiang Lv[2] · Shaowen Zhang[1]

Received: 1 October 2015 / Accepted: 18 January 2016 / Published online: 15 February 2016

Abstract The mechanism and kinetics for the reaction of benzyl alcohol with OH radical have been studied by using the hybrid meta-density functional theory (M06-2X) and the conventional transition state theory. The results show that six van der Waals complexes are formed firstly as the OH radical approaches benzyl alcohol from different directions, and then the OH radical may abstract the H atoms from the $–CH_2OH$ group and the benzene ring, or adduct to C atoms of the benzene ring. Among all the possible reaction channels, the alkyl hydrogen abstraction from the $–CH_2OH$ group and the ipso and ortho-C addition are dominant. The calculated overall rate constant is 2.61×10^{-11} cm^3 $molecule^{-1}$ s^{-1}, and the branching ratios of the hydrogen abstraction and the addition reactions are 0.23 and 0.77, respectively, at 298 K. As the temperature rises from 250 to 400 K, the branching ratio of the hydrogen abstraction reaction increases while that of the addition reaction decreases. The calculation results are in good agreement with the available experimental values.

Keywords Benzyl alcohol · van der Waals complex · Reaction mechanism · Kinetics · Branching ratio

Electronic supplementary material The online version of this article (doi:10.1007/s00214-016-1811-2) contains supplementary material, which is available to authorized users.

✉ Shaowen Zhang
swzhang@bit.edu.cn

[1] Key Laboratory of Cluster Science of Ministry of Education, School of Chemistry, Beijing Institute of Technology, Beijing 100081, People's Republic of China

[2] College of Chemical Engineering, Shijiazhuang University, Shijiazhuang 050035, People's Republic of China

1 Introduction

Aromatic compounds, a main source of the nonmethane volatile organic compounds, are ubiquitous in the atmosphere. In the presence of NO_x (NO_2 + NO), the degradation of aromatics can form ozone and a number of photooxidants, and has a high propensity to the formation of secondary organic aerosols (SOAs), which affect the air quality seriously [1–3].

Many aromatic compounds are expected to react very rapidly with the OH radical, O_3, and NO_3 radical due to the C=C double bonds contained in them. It is well known that OH radical is an important atmospheric oxidation species, and amounts of theoretical and experimental studies on the reactions of OH with benzene [4–6], toluene [7–9], xylenes [10, 11], cresol [12], and benzaldehyde [13] have been carried out.

Benzyl alcohol, an aromatic primary alcohol, is mainly used as a solvent in paint stripper and as an intermediate for the synthesis of target molecules used in pharmaceuticals, cosmetics, preservatives, and flavoring and fragrance agents. Due to the potential influence of benzyl alcohol to atmosphere, some experiments have been carried out to determine the rate constant of the reactions of benzyl alcohol with OH, O_3, and NO_3. Harrison and Wells [14] measured the rate constant for the reaction of the OH radical with benzyl alcohol, which is predicted to be $(2.8 \pm 0.7) \times 10^{-11}$ cm^3 $molecule^{-1}$ s^{-1} at 297 K and 1 atm total pressure, and they obtained the upper limit of the bimolecular rate constant of benzyl alcohol with O_3, 6×10^{-19} cm^3 $molecule^{-1}$ s^{-1}. The rate constant and products of the reaction NO_3 with benzyl alcohol have also been measured by Harrison and Wells [15], the observed rate constant is $(4.0 \pm 1.0) \times 10^{-15}$ cm^3 $molecule^{-1}$ s^{-1}, and benzaldehyde ($(C_6H_5)C(O)H$) was the only derived product observed, which is formed by the alkyl hydrogen abstraction of NO_3 from benzyl alcohol and followed by the

reaction of O_2 with $(C_6H_5)CH(\cdot)(OH)$ radical. Bernard et al. [16] reported the rate constant of the benzyl alcohol + OH reaction, $(2.8 \pm 0.4) \times 10^{-11}$ cm^3 molecule^{-1} s^{-1}, which is consistent with the value measured by Harrison et al. [14]; by identifying the reaction products, they concluded that benzaldehyde is originated from the H-abstraction from the $-CH_2OH$ group with a yield of (24 ± 5) %, and the remaining 75 % products of the reaction are originated from the addition of the OH radical to the aromatic ring.

For the benzyl alcohol + OH reaction, the rate constant, the product branching ratios, and the hydrogen abstraction sites of OH from benzyl alcohol have been obtained by experiments; however, the addition sites of OH to the benzene ring remain unclear, and a detailed theoretical study is necessary to give a complete reaction mechanism and to analyze the subtle balance between the different reaction channels. With this aim, we calculated the reaction potential energy surface by considering all the possible hydrogen abstraction and addition reactions between benzyl alcohol and the OH radical. Based on the energetic, structural, and vibrational results by the density functional theory, the conventional transition state method was employed to predict the rate constants and the branching ratio of the competing abstraction and addition reactions.

2 Computational method

2.1 Electronic structure calculations

All the stationary points (minima and first-order saddle points) were optimized by using the hybrid meta-density functional theory M06-2X [17] with the 6-311+g(2df,2pd) basis set. The good performance of the M06-2X functional on the main-group thermochemistry, the kinetics, and also on the prediction of noncovalent interactions has been tested by Truhlar et al. [17, 18], and the reliability of the calculation results by M06-2X functional has also been verified by theoretical kinetics studies [19–21]. The harmonic vibrational frequencies of these stationary points were computed at the same level of electronic structure calculations, and the local minima and transition states (TS) were identified by the number of imaginary frequencies (NIMAG = 0 or 1, respectively). Connections of the transition state between the designated minima were confirmed by the intrinsic reaction coordinate (IRC) calculations [22]. The spin contamination on the complexes and transition states has been checked, and the corresponding $\langle S^2 \rangle$ values for the M06-2X calculations are <0.78 before projection and very close to 0.75 after projection.

In order to give more reliable energetic results for the subsequent kinetics calculation, the multi-level energy calculations (denoted as ML) [23] were used to calculate the energy of every stationary point based on the optimized geometries at the M06-2X/6-311+g(2df,2pd) level of theory. The ML method employs a combination of QCISD(T) and MP2 methods and can be expressed as

$$\begin{aligned} E_{\mathrm{ML}} = {} & E[\mathrm{QCISD(T)/cc\text{-}pVTZ}] + (E[\mathrm{QCISD(T)/cc\text{-}pVTZ}] \\ & - E[\mathrm{QCISD(T)/cc\text{-}pVDZ}]) \times 0.46286 \\ & + E[\mathrm{MP2/cc\text{-}pVQZ}] + (E[\mathrm{MP2/cc\text{-}pVQZ}] \\ & - E[\mathrm{MP2/cc\text{-}pVTZ}]) \times 0.69377 - E[\mathrm{MP2/cc\text{-}pVTZ}] \\ & - (E[\mathrm{MP2/cc\text{-}pVTZ}] - E[\mathrm{MP2/cc\text{-}pVDZ}]) \times 0.46286 \end{aligned}$$

This energy refinement scheme has been tested suitable for reaction systems involving radicals and can give more accurate energetics for the kinetics calculation.

All of the above calculations have been carried out by using the Gaussian 09 program package [24].

There exist several reaction complexes (RCs) in the reaction of OH with benzyl alcohol. The noncovalent interactions in the RCs were analyzed by the molecular electrostatic potential (ESP) [25]. In this work, the molecular electrostatic potentials on the 0.001 a.u. electron density isosurface of benzyl alcohol and OH radical have been obtained and depicted by using the WFA surface analysis suite [26].

2.2 Rate constant calculations

The rate constants of all the reaction channels are computed by using the conventional transition state theory (TST) [27] as implemented in TheRate program [28], and the tunneling corrections are taken into account for the hydrogen abstraction channels with the unsymmetrical Eckart potentials. As in most radical-molecule reactions, all the hydrogen abstraction and OH addition channels consist of a reversible first step involving the barrierless formation of a reaction complex (RC) in the entrance channel, followed by the irreversible formation of products, as shown in Eqs. (1) and (2):

$$\text{Step 1: } C_6H_5CH_2OH + OH \leftrightarrow \text{Complex} \tag{1}$$

$$\text{Step2 : Complex} \rightarrow \text{Products} \tag{2}$$

The complex mechanism for the radical-molecule reactions was first proposed by Singleton and Cvetanovic [29] and has been used successfully in quantum chemistry TST calculations [8, 9, 13, 30–34]. If k_1 and k_{-1} are, respectively, the forward and reverse rate constants for the first step and k_2 is the rate constant for the second step, a steady-state analysis leads to a rate constant of the overall reaction, which can be approximated as Eq. (3):

$$k = \frac{k_1}{k_{-1}} k_2 = K_{\mathrm{eq}} k_2 \tag{3}$$

where K_{eq} is the equilibrium constant between the isolated reactants and the reaction complex. Applying basic statistical thermodynamic principles, K_{eq} can be written as Eq. (4):

$$K_{eq} = \frac{Q_{RC}}{Q_{C_6H_5CH_2OH} Q_{OH}} \exp\left[(E_R - E_{RC})/RT\right] \quad (4)$$

where $Q_{C_6H_5CH_2OH}$, Q_{OH}, and Q_{RC} are the partition functions of reactants benzyl alcohol, OH, and the reaction complex, respectively; E_R and E_{RC} are the respective total energies of the reactants and the reaction complex, R is the ideal gas constant, and T is the absolute temperature.

The rate constant k_2 can be evaluated according to the conventional transition state theory Eq. (5):

$$k_2 = \kappa\sigma \frac{k_B T}{h} \frac{Q_{TS}}{Q_{RC}} \exp\left[(E_{RC} - E_{TS})/RT\right] \quad (5)$$

where κ is the tunneling factor, which is calculated assuming an unsymmetrical, one-dimensional Eckart function barrier [35]; sigma is the symmetry factor, i.e., the reaction path degeneracy that accounts for the number of equivalent reaction paths. Considering the geometry structure of benzyl alcohol with C_1 symmetry, we studied the hydrogen abstraction and addition reactions as the OH radical attacks the H or C atoms in the direction above and below the benzyl ring, respectively. Thus, the symmetry factor was taken to be 1 for every calculated hydrogen abstraction and addition reaction channel; k_B is the Boltzmann constant, h is the Planck constant, and Q_{TS} and E_{TS} are the transition state partition function and total energy, respectively. Then the effective rate coefficient of each channel can be written as Eq. (6):

$$k = \kappa\sigma \frac{k_B T}{h} \frac{Q_{TS}}{Q_{C_6H_5CH_2OH} Q_{OH}} \exp\left[(E_R - E_{TS})/RT\right] \quad (6)$$

Like the approach previously used to evaluate the OH radical reactions with several volatile organic compounds (VOCs) [8, 9, 13, 30–34], we assume that the reaction complex undergoes collisional stabilization and the reaction occurs at the high-pressure limit.

An accurate evaluation of the partition functions Q is essential to the reliability of the calculated rate constant. Some low-frequency torsional modes are in fact hindered internal rotations, and when the rotational barrier is smaller than about 3.0 kcal mol^{-1}, these modes should be removed from the vibrational partition function of the corresponding species and replaced with the hindered rotor partition function (Q_{HR}). So we calculated the rotational barrier of some low-frequency torsional modes to determine whether they should be treated as hindered internal rotations. We adopt the analytical approximation to Q_{HR} for a one-dimensional hindered internal rotation proposed by Ayala and Schlegel [36].

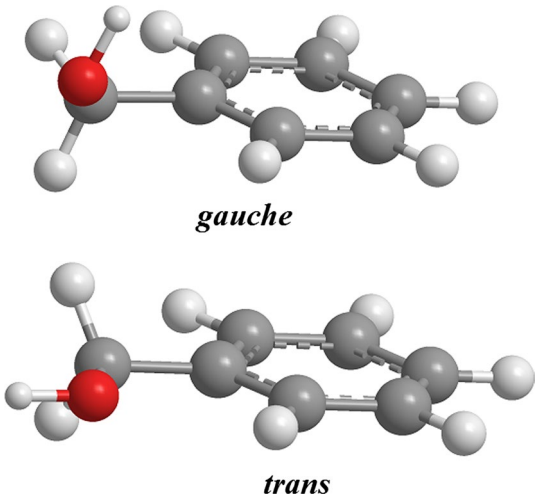

Fig. 1 Structures of the *gauche* and *trans* conformers of benzyl alcohol

3 Results and discussion

3.1 Reaction mechanism

3.1.1 Analysis of the geometries of benzyl alcohol

The calculation results show that benzyl alcohol exhibits two stable conformers, the *gauche* and *trans* forms (Fig. 1), with the OH group oriented toward or away from the benzene ring, and both the *gauche* and *trans* forms have been predicated by the previous theoretical calculations [37–39]. The calculated energy of the *gauche* form is 0.51 kcal mol^{-1} lower than that of the *trans* form at the M06-2x/6-311+g(2df,2pd) level of theory. Furthermore, only the *gauche* form has been positively identified in experimental studies [40] to date, so the *gauche* conformer was taken into account for the mechanism and kinetics study in the reaction of benzyl alcohol with OH radical.

3.1.2 Analysis of the reaction complexes

As reactants approach each other, several shallow minima, corresponding to the reaction complexes, are located. The existence and structure of such minima have been discussed in many previous theoretical studies [8, 31, 32, 41–43]. These reaction complexes result from van der Waals interactions, and they play an important role in the evaluation of the reaction barrier height, which have a strong effect on the tunneling correction. The geometries of the RCs, optimized with the M06-2X/6-311+g(2df,2pd) method, are shown in Fig. 2. To analyze the noncovalent interactions in the complexes, the molecular ESPs on the 0.001 a.u. electron density isosurfaces of benzyl alcohol and OH

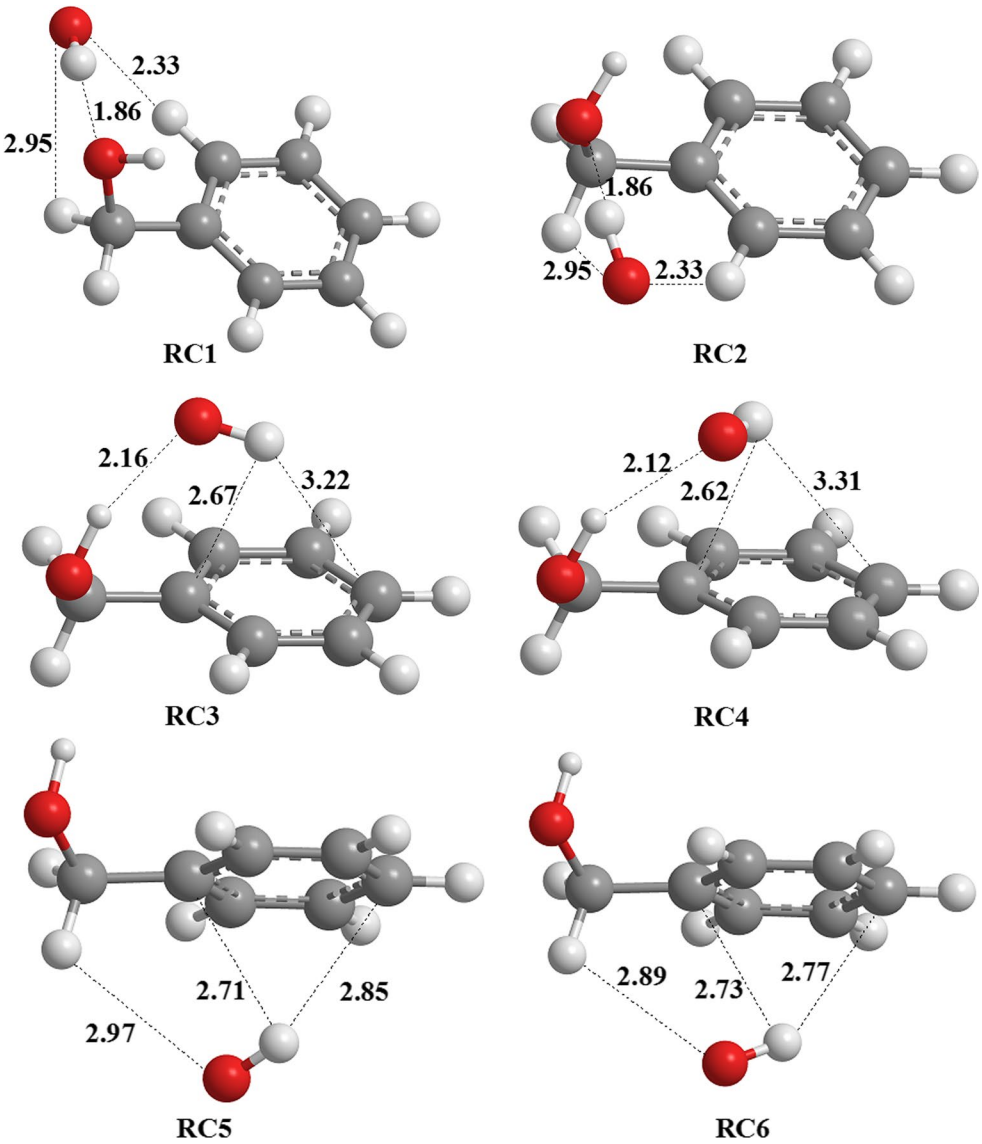

Fig. 2 Optimized geometries of the van der Waals complexes. The unit of the inter-atomic distances is given in angstrom (Å)

were computed and are shown in Fig. 3. For benzyl alcohol, the positive regions of the contour maps are located at positions corresponding to the H atoms outer side along the extension of the O–H or C–H bonds; there are two types of negative regions on the contour maps: one is located just above and below the benzene ring and the other along the lone electron pairs orientation of the O atom. For OH radical, the positive and negative ESP regions are located at the H and O atoms outer side, respectively. In the complexes RC1 and RC2, the H atom of OH radical is attracted by the negative region of the O atom in the hydroxyl group of benzyl alcohol, and meanwhile, there is a weak interaction between the O atom of OH radical and the ortho-H atom of the benzene ring, and the O···H distances are 1.86 and 2.33 Å, respectively, as shown in Fig. 3a. The OH radical may approach the benzyl alcohol in the direction above (RC3 and RC4) and below (RC5 and RC6) the benzyl ring, and the words "above" and "below" refer to the side of the benzyl ring where the OH group is located or not, respectively. The structures of RC3–RC6 are different from those of RC1 and RC2. In the complexes RC3–RC6, the H atom of OH radical points toward the negative region of the aromatic ring due to a π-type hydrogen bond interaction [40], and meanwhile, the O atom of OH radical points toward the positive ESP regions of the H atoms in the $–CH_2OH$ group of benzyl alcohol, as shown in Fig. 3b and c. In RC3–RC6, the distances of the H atom from the center of the aromatic ring are about 2.5 Å, and the O···H distances are about 2.16, 2.12, 2.97, and 2.89 Å from RC3 to RC6, respectively. The O···H distances in RC1 and RC2 are shorter than those in RC3–RC6, so the energies of RC1 and RC2 are lower than those of RC3–RC6. Starting from these RCs, the OH radical and benzyl alcohol will proceed via hydrogen abstraction and addition reactions.

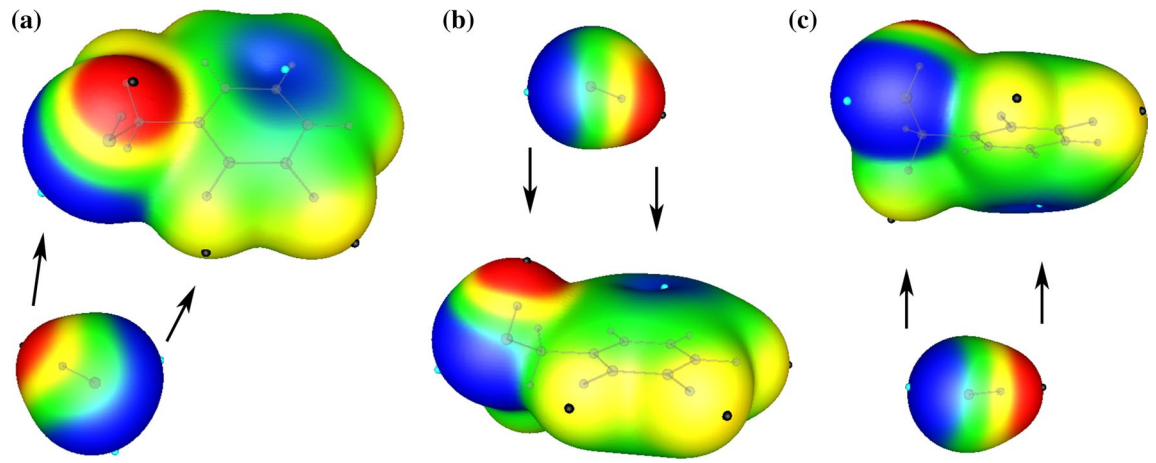

Fig. 3 Schematic diagram of the formation of the complexes by the noncovalent interactions between benzyl alcohol and the OH radical: **a** for RC1 and RC2, **b** for RC3 and RC4, and **c** for RC5 and RC6. Electrostatic potentials are taken on the 0.001 a.u. contour of the molecular electron density for benzyl alcohol and the OH radical. Color ranges (unit in kcal mol^{-1}): *red* more positive than 20; *yellow* 5–20; *green* −10 to 5; *blue* more negative than −10

3.1.3 The hydrogen abstraction and addition channels

For the reaction of OH with benzyl alcohol, all the possible reaction channels have been considered. The OH radical may abstract the H atom from the $–CH_2OH$ group or from the different sites of the benzene ring, forming a water molecule and the corresponding radical, and the OH radical may adduct to the benzene ring. As mentioned above, benzyl alcohol is not symmetric, and the OH radical may approach the benzyl alcohol in the direction above and below the benzyl ring, so for the addition channels, the respective transition states are defined as TSadd*i*a and TSadd*i*b (i = 1–6), and the letters "a" and "b" are used to denote "above" and "below," respectively; for the hydrogen abstraction channels from the benzene ring, the H atom of the OH radical may point up and down with the O–H bond vertical to the benzene ring approximatively, and the respective transition states are defined as TSabs*i*a and TSabs*i*b (i = 2–6). As shown in Fig. 4, all the hydrogen abstraction and addition reactions initiate from a certain RC. For clarity and simplicity, not all the geometries of the transition states are portrayed in Fig. 4, and the corresponding H and C atoms are labeled to denote the sites of the hydrogen abstraction and addition reaction. OH radical approaches benzyl alcohol from the side of the hydroxymethyl group forming RC1 and RC2, and then OH abstracts the alkyl hydrogen atoms H7 and H8, respectively, and the OH in RC2 may also abstract H6 atom on benzene ring. As the OH radical approaches the benzene ring from above, the reaction complexes RC3 and RC4 are formed. The OH in RC3 may abstract the H2, H3, and H4 atoms or adduct to the C1, C2, C3, and C4 atoms, while the OH in RC4 may abstract the H5 and H9 atoms or adduct to the C5 and C6 atoms. As the OH radical approaches the benzene ring from below, the reaction complexes RC5 and RC6 are formed. Starting from RC5, the OH radical may abstract the H2, H3, and H4 atoms or adduct to the C1, C2, C3, and C4 atoms of benzene ring, while the OH in RC6 may abstract the H5 and H6 atoms or adduct to the C5 and C6 atoms. Cartesian coordinates and frequencies of all the reactants, RCs, and transition states are given in the supplementary materials.

In order to obtain more accurate energetic information for the subsequent kinetics calculation, the energies of all the stationary points were calculated by using the ML method based on the M06-2X/6-311+g(2df,2pd) optimized geometries. The energies of the reaction complexes RC1, RC2, RC3, RC4, RC5, and RC6 are −5.1, −5.1, −4.5, −4.2, −2.3, −2.4 kcal mol^{-1} relative to that of the reactants, respectively. The relative energies of all the transition states and products are listed in Table 1, and the total energy of the reactants is set as zero for reference.

From Table 1, we can see that for the addition channels, the relative energies of TSadd1a, TSadd2a, TSadd6a, TSadd1b, TSadd2b, and TSadd6b are −3.1, −2.6, −2.8, −0.2, 0.2, and 0.1 kcal mol^{-1}, respectively, which are lower than or almost equal to that of the reactants. So the additions to the ipso and ortho-C atoms are dominant; moreover, the OH radical adducts to the benzene ring from above is more favorable than from below. For the addition transition states, the O atom of OH radical attacks the C atom of benzene ring, and the O···C distances in TSadd1a–TSadd6a (TSadd1b–TSadd6b) are all about 2.0 Å. It is found that there exist interactions between the O atom of OH radical and the H atom of the hydroxymethyl group in the ipso and ortho-addition TSs but not in

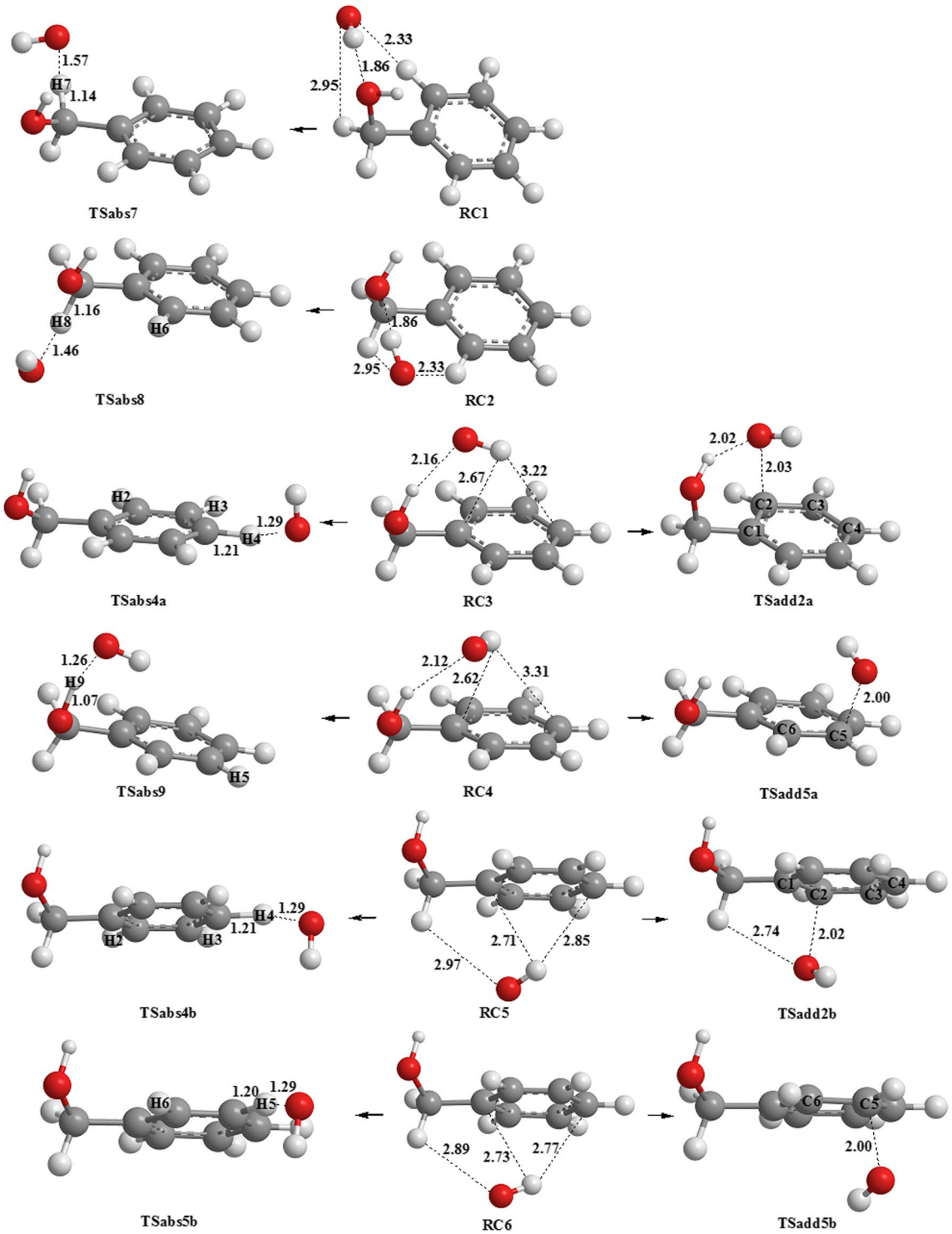

Fig. 4 Optimized geometries of the transition states. The unit of the inter-atomic distances is given in angstrom (Å)

the meta- and para-addition TSs, which explains why the energies of TSadd1a (TSadd1b), TSadd2a (TSadd2b), and TSadd6a (TSadd6b) are lower than those of TSadd3a (TSadd3b), TSadd4a (TSadd4b), and TSadd5a (TSadd5b). The O···H (hydroxy-H in $-CH_2OH$ group) distances in TSadd1a, TSadd2a, and TSadd6a are about 2.0 Å, and the O···H (alkyl-H in $-CH_2OH$ group) distances in TSadd1b, TSadd2b, and TSadd6b are about 2.5–2.7 Å. The shorter O···H interaction distances result in the lower energies of TSadd1a, TSadd2a, and TSadd6a compared to those of

Table 1 The relative energies of all the transition states and products calculated at the ML//M06-2X/6-311+g(2df,2pd) level of theory (including ZPE, unit: kcal mol^{-1})

H-abstraction channels				Addition channels			
TSs	E_{rel}	Products	E_{rel}	TSs	E_{rel}	Products	E_{rel}
TSabs2a	3.9	Pabs2a	−6.5	TSadd1a	−3.1	Padd1a	−21.5
TSabs3a	4.1	Pabs3a	−6.5	TSadd2a	−2.6	Padd2a	−19.4
TSabs4a	4.4	Pabs4a	−6.0	TSadd3a	1.4	Padd3a	−17.3
TSabs5a	4.3	Pabs5a	−6.5	TSadd4a	1.3	Padd4a	−17.2
TSabs6a	2.0	Pabs6a	−5.7	TSadd5a	1.5	Padd5a	−16.8
TSabs2b	3.9	Pabs2b	−6.5	TSadd6a	−2.8	Padd6a	−18.7
TSabs3b	4.3	Pabs3b	−6.5	TSadd1b	−0.2	Padd1b	−20.0
TSabs4b	4.2	Pabs4b	−6.0	TSadd2b	0.2	Padd2b	−18.1
TSabs5b	4.3	Pabs5b	−6.5	TSadd3b	1.2	Padd3b	−17.4
TSabs6b	4.9	Pabs6b	−5.7	TSadd4b	1.3	Padd4b	−17.4
TSabs7	−0.4	Pabs7	−35.3	TSadd5b	1.6	Padd5b	−16.9
TSabs8	−0.4	Pabs8	−35.3	TSadd6b	0.1	Padd6b	−18.1
TSabs9	2.1	Pabs9	−13.4				

Table 2 The calculated rate constant for every possible reaction channel at 298 K (unit: 10^{-12} cm^3 $molecule^{-1}$ s^{-1})

Abs	H2a	H2b	H3a	H3b	H4a	H4b	H5a	H5b	H6a	H6b	H7	H8	H9
k_i	0.003	0.004	0.005	0.001	0.002	0.002	0.002	0.002	0.04	0.001	1.83	4.11	0.05
Add	C1a	C1b	C2a	C2b	C3a	C3b	C4a	C4b	C5a	C5b	C6a	C6b	
k_i	8.58	0.17	5.05	0.07	0.07	0.04	0.05	0.03	0.03	0.02	5.90	0.11	

TSadd1b, TSadd2b, and TSadd6b. So the addition of OH radical to the benzene ring from above is more competitive. For the hydrogen abstraction channels, it is obvious that the alkyl-H (H7 and H8) abstraction from the $–CH_2OH$ group is dominant, the relative energies of the corresponding transition states (TSabs7, TSabs8) and products (Pabs7, Pabs8) are −0.4 and −35.3 kcal mol^{-1}, respectively, while all the other abstraction channels need to get over some energy barriers. This can be explained by the existence of the conjugated π bond π_8^9 in the alkyl hydrogen abstraction products, which results in the lower energies of Pabs7 and Pabs8. These results will be confirmed by the subsequent rate constants' calculation.

3.2 Rate constants calculations

As discussed in the Computational method Section, the rotational barriers of some low-frequency torsional modes need to be calculated to determine whether they should be treated as rotations or vibrations. We obtain these rotational barriers by scanning the PES of the torsion dihedral angles at the M06-2X/6-311+g(2df,2pd) level of theory. For benzyl alcohol, all degrees of freedom are optimized except the rotational dihedral angle being scanned. It is found that the internal rotational barrier heights of OH and CH_2OH groups in benzyl alcohol are lower than 3 kcal mol^{-1}, so both of the two internal rotations should be taken into account to correct the partition functions of benzyl alcohol. For the transition states, in addition to the rotational dihedral angle being scanned, the lengths of the breaking and forming bonds are fixed at the TS values during optimization. For the alkyl-H-abstraction TSs, the internal rotational barriers of the $CH_2OH\cdots OH$ group and two OH groups were calculated, and all of them are no more than 3 kcal mol^{-1}, and these motions were considered as hindered internal rotations. For the addition TSs, the internal rotation of the CH_2OH group and two OH groups were analyzed. The internal rotational barrier heights of the three groups in the ipso and ortho-addition transition states TSadd1a (TSadd1b), TSadd2a (TSadd2b), and TSadd6a (TSadd6b) are found to be higher than 3 kcal mol^{-1}, so they were considered as vibrations. The analysis of the internal rotational barriers of low-frequency torsional modes in other transition states is given in the supplementary materials.

The rate constants and branching ratios are calculated at the 250–400 K temperature range. The rate constants of all the possible reaction channels at 298 K are listed in Table 2. As shown in Table 2, the rate constants for the alkyl-H (H7 and H8) abstraction are 1.83×10^{-12} and 4.11×10^{-12} cm^3 $molecule^{-1}$ s^{-1}, respectively, which are much larger than those of other hydrogen abstraction channels. The addition reaction occurs mainly at the ipso and ortho-carbon

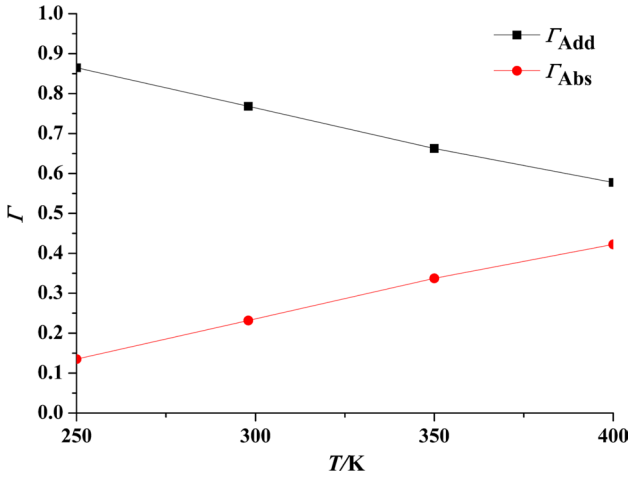

Fig. 5 Temperature dependence of the branching ratios of the abstraction channels and the addition channels

atoms, and the rate constants for the OH addition to the C1, C2, and C6 atoms of benzene ring from above (below) are 8.58×10^{-12} (0.17×10^{-12}), 5.05×10^{-12} (0.07×10^{-12}), and 5.90×10^{-12} (0.11×10^{-12}) cm^3 $molecule^{-1}$ s^{-1}, respectively. These results are in good agreement with the conclusion from energetics.

The overall rate constant ($k_{overall}$) of benzyl alcohol + OH reaction can be calculated as the sum of the rate constants of all the possible channels. The branching ratios for the hydrogen abstraction and addition reactions are calculated by Eqs. (7) and (8).

$$\Gamma_{Abs} = \frac{k_{Abs}}{k_{overall}} \tag{7}$$

$$\Gamma_{Add} = \frac{k_{Add}}{k_{overall}} \tag{8}$$

where k_{Abs} and k_{Add} are the sum of the rate constants of all the hydrogen abstraction channels and all the addition channels, respectively. At 298 K, $k_{overall}$ is 2.61×10^{-11} cm^3 $molecule^{-1}$ s^{-1}, and the branching ratios of the hydrogen abstraction and addition reactions are 0.23 and 0.77, respectively. The overall rate constant reported by experiment is about 2.8×10^{-11} cm^3 $molecule^{-1}$ s^{-1} [14, 16], and the respective experimental branching ratios for the hydrogen abstraction and addition reactions are about 0.25 and 0.75 [16]. Thus, the theoretical calculations are consistent with the experimental results.

The branching ratios for the hydrogen abstraction and addition channels are plotted in Fig. 5 as a function of temperature. As shown in Fig. 5, the branching ratio of the hydrogen abstraction reaction increases while that of the addition reaction decreases from 0.86 to 0.58 as the temperature changes from 250 to 400 K.

4 Conclusions

Based on the ML//M06-2X/6-311+g(2df, 2pd) level of theory, the reaction mechanism for the benzyl alcohol + OH reaction has been investigated. The rate constants are calculated by the conventional transition state theory with the Eckart tunneling corrections. Several conclusions can be drawn from the above calculations. (1) There exist van der Waals complexes between benzyl alcohol and the OH radical, both the hydrogen abstraction and addition reactions initiate from these complexes. (2) The dominant reaction channels were determined to be the alkyl hydrogen abstraction from the $–CH_2OH$ group and the addition of OH to the ipso and ortho-C atoms of benzene ring. (3) The calculated overall rate constant is 2.61×10^{-11} cm^3 $molecule^{-1}$ s^{-1}, and the branching ratios of the hydrogen abstraction and the addition reactions are, respectively, about 23 and 77 % at the temperature of 298 K. (4) The branching ratio of the hydrogen abstraction reaction increases as the temperature rises from 250 to 400 K, and the branching ratio of the addition reaction decreases accordingly in the same temperature range.

Acknowledgments This work is supported by the National Natural Science Foundation of China (No. 21173022) and the foundation of Shijiazhuang University (No. 14BS003, 10ZDA001).

References

1. Bloss C, Wagner V, Jenkin ME, Volkamer R, Bloss WJ, Lee JD, Heard DE, Wirtz K, Martin-Reviejo M, Rea G, Wenger JC, Pilling MJ (2005) Atmos Chem Phys 5:641–664
2. Derwent RG, Jenkin ME, Saunders SM (1996) Atmos Environ 30:181–199
3. Forstner HJL, Flagan RC, Seinfeld JH (1997) Environ Sci Technol 31:1345–1358
4. Atkinson R, Arey J (2003) Chem Rev 103:4605–4638
5. Hollman DS, Simmonett AC, Schaefer HF (2011) Phys Chem Chem Phys 13:2214–2221
6. Tokmakov IV, Lin MC (2002) J Phys Chem A 106:11309–11326
7. Suh I, Zhang R, Molina LT, Molina MJ (2003) J Am Chem Soc 125:12655–12665
8. Uc VH, Alvarez-Idaboy JR, Galano A, Garcia-Cruz I, Vivier-Bunge A (2006) J Phys Chem A 110:10155–10162
9. Uc VH, Alvarez-Idaboy JR, Galano A, Vivier-Bunge A (2008) J Phys Chem A 112:7608–7615
10. Birdsall AW, Elrod MJ (2011) J Phys Chem A 115:5397–5407
11. Noda J, Volkamer R, Molina MJ (2009) J Phys Chem A 113:9658–9666
12. Wu P, Guo S, Li S, Tao F-M (2011) Comput Thero Chem 971:51–57
13. Iuga C, Galano A, Vivier-Bunge A (2008) ChemPhysChem 9:1453–1459
14. Harrison JC, Wells JR (2009) Atmos Environ 43:798–804
15. Harrison JC, Wells JR (2012) Int J Chem Kinet 44:778–788
16. Bernard F, Magneron I, Eyglunent G, Daele V, Wallington TJ, Hurley MD, Mellouki A (2013) Environ Sci Technol 47:3182–3189

17. Zhao Y, Truhlar DG (2008) Theor Chem Acc 120:215–241
18. Zhao Y, Truhlar DG (2008) Acc Chem Res 41:157–167
19. Piletic IR, Edney EO, Bartolotti LJ (2013) Phys Chem Chem Phys 15:18065
20. Balaganesh M, Dash MR, Rajakumar B (2014) J Phys Chem A 118:5272–5278
21. Srinivasulu G, Rajakumar B (2015) J Phys Chem A 119:9294–9306
22. Gonzalez C, Schlegel HB (1989) J Chem Phys 90:2154–2161
23. Miller JA, Klippenstein SJ (2003) J Phys Chem A 107:2680–2692
24. Frisch MJ et al (2013) Gaussian 09, Revision D01. Gaussian Inc, Wallingford, CT
25. Li W, Zeng Y, Zhang X, Zheng S, Meng L (2014) Phys Chem Chem Phys 16:19282–19289
26. Bulat FA, Toro-Labbe A, Brinck T, Murray JS, Politzer P (2010) J Mol Model 16:1679–1991
27. Truhlar DG, Garrett BC, Klippenstein SJ (1996) J Phys Chem 100:12771–12800
28. Duncan WT, Bell RL, Truong TN (1998) J Comput Chem 19:1039–1052
29. Singleton DL, Cvetanovic RJ (1976) J Am Chem Soc 98:6812–6819
30. Alvarez-Idaboy JR, Mora-Diez N, Boyd RJ, Vivier-Bunge A (2001) J Am Chem Soc 123:2018–2024
31. Alvarez-Idaboy JR, Mora-Diez N, Vivier-Bunge A (2000) J Am Chem Soc 122:3715–3720
32. Galano A, Alvarez-Idaboy JR, Ruiz-Santoyo ME, Vivier-Bunge A (2002) J Phys Chem A 106:9520–9528
33. Olivella S, Sole A (2008) J Chem Theory Comput 4:941–950
34. Vega-Rodriguez A, Alvarez-Idaboy JR (2009) Phys Chem Chem Phys 11:7649–7658
35. Truong TN, Truhlar DG (1990) J Chem Phys 93:1761–1769
36. Ayala PY, Schlegel HB (1998) J Chem Phys 108:2314–2325
37. Dessent CEH, Geppert WD, Ullrich S, Muller-Dethlefs K (2000) Chem Phys Lett 319:375–384
38. Mons M, Robertson EG, Simons JP (2000) J Phys Chem A 104:1430–1437
39. Utzat K, Restrepo AA, Bohn RK, Michels HH (2004) Int J Quantum Chem 100:964–972
40. Trætterberg M, Østensen H, Ragnhild S (1980) Acta Chem Scand 34:449–454
41. Sosa C, Schlegel HB (1987) J Am Chem Soc 109:4193–4198
42. Uc VH, García-Cruz I, Hernández-Laguna A, Vivier-Bunge A (2000) J Phys Chem A 104:7847–7855
43. Sekušak S, Sabljić A (1997) Chem Phys Lett 272:353–360